Ecography

E7587
Louzao, M., Aumont, O., Hothorn, T., Wiegand, T. and Weimerskirch, H. 2012. Foraging in a changing environment: habitat shifts of an oceanic predator over the last half century. – Ecography 35: xxx–xxx.

Supplementary material

APPENDIX 1. TRACKING ANALYSIS

To assess the foraging habitat, the albatross tracking data were analysed by means of the First Passage Time (FPT). This approach is based on identifying area restricted search behaviour along the foraging trips which is indicative of foraging. In this case birds alter their movement rates and/or frequencies of turns in response to heterogeneously distributed resources (Fauchald and Tveraa 2003). We detected the maximum scale at which albatrosses concentrated their foraging effort, as well as nested spatial scales following Fauchald and Tveraa (2003), Pinaud and Weimerskirch (2005) and Weimerskirch et al. (2007). In order to identify areas where individuals showed area restricted search behaviour (i.e. foraging in our case indicated by high FPT values), a first passage time value threshold was determined according to its multimodal distribution: area-restricted search zones corresponded to the mode of higher first passage time values (see Fig. S1 in Pinaud and Weimerskirch 2007). By inspecting the first passage time/travelling time plot, we selected the spatial locations of high search effort (i.e. high FPT values). The multimodal distribution of each foraging trip was inspected manually to objectively select the threshold value specific for each individual. Note that the entire foraging trip was analysed following (Fauchald and Tveraa 2003, Pinaud and Weimerskirch 2005) and consequently we did not remove locations with high FPT values occurring at night (Pinaud and Weimerskirch 2007).

Next, a categorical binomial variable was assigned to each cell, indicating whether at least one 'foraging' event occurred within a given cell of 1º or not (e.g. 'not foraging'). The 1º spatial resolution corresponds approximately to a cell size of approximately 80 × 110 km where we summarised foraging events. Given this coarse spatial resolution a small change in the threshold values would rarely change the number of cells identified as "foraging" or "not foraging". Overall, the total number of visited cells per trip ranged between 6 and 198, and "foraging" records between 4 and 174 representing between the 3.13% and 75% of the total locations per foraging trip (see details of the binomial response variable by foraging trip in Table S1).

References

Fauchald, P. and Tveraa, T. 2003. Using first-passage time in the analysis of area-restricted search and habitat selection. - Ecology 84: 282-288.

Pinaud, D. and Weimerskirch, H. 2005. Scale-dependent habitat use in a long-ranging central place predator. - J. Anim. Ecol. 74: 852-863.

Pinaud, D. and Weimerskirch, H. 2007. At-sea distribution and scale-dependent foraging behaviour of petrels and albatrosses: a comparative study. – Ecology 76: 9-19.

Weimerskirch, H. et al. 2007. Does prey capture induce area-restricted search? A fine-scale study using GPS in a marine top predator, the Wandering Albatross. – Am. Nat. 170: 734-743.

Table A1. Detailed listing of all trips and the number of foraging and non foraging records.

Trip identification	# records "Foraging"	# records "Not foraging"	Total records	Foraging (%)
11376_2001_1	6	154	160	3.75
11378_2001_1	4	25	29	13.79
11378_2001_2	8	19	27	29.63
11378_2001_4	9	40	49	18.37
25071_2001_1	16	8	24	66.67
25076_2001_2	24	174	198	12.12
8196_2001_1	21	48	69	30.43
8196_2001_2	17	88	105	16.19
8337_2001_1	5	27	32	15.63
8337_2001_2	8	8	16	50.00
BS10304_11378_1999	7	39	46	15.22
BS10708_25074_1999	8	45	53	15.09
BS10759_25074_1999	4	23	27	14.81
BS10770_25076_1998	6	15	21	28.57
BS10775_25075_1999	4	49	53	7.55
BS10809_11377_1998	4	30	34	11.76
BS10860_25072_1998	11	29	40	27.50
BS11673_25070_1999	4	2	6	66.67
BS11686_11380_1999	6	2	8	75.00
BS11816_25070_1999	9	34	43	20.93
BS11855_11376_1999	10	17	27	37.04
BS12307_11378_1999	21	119	140	15.00
BS12340_25073_1999	2	53	55	3.64
BS12988_25071_1999	9	35	44	20.45
BS156_25070_1998	4	14	18	22.22
BS20035_25071_2000_1	10	34	44	22.73
BS20051_11377_1999	12	57	69	17.39
BS20053_25072_1999	2	46	48	4.17
BS21133_25071_1999	5	40	45	11.11
BS21165_25073_1998	6	38	44	13.64
BS21799_25075_1999	9	27	36	25.00
BS4592_25069_1998	4	39	43	9.30
BS4632_25076_2000	17	79	96	17.71
BS4770_25071_1999	6	54	60	10.00
BS4790_11378_1999	10	18	28	35.71
BS4796_25073_1998	8	23	31	25.81
BS4898_11376_1998	6	4	10	60.00
BS4959_11376_1998	19	11	30	63.33
BS5151_25076_1999	6	68	74	8.11
BS5328_11376_1999	2	62	64	3.13
BS6105_25076_1999	21	55	76	27.63
BS6239_11380_1999	1	27	28	3.57
BS6240_25071_1998	3	16	19	15.79
BS6297_25073_1998	5	2	7	71.43
BS6467_11377_1998	6	15	21	28.57

BS6575_25070_1999	11	12	23	47.83
BS6663_25071_2000	4	5	9	44.44
BS7625_11377_1999	11	83	94	11.70
BS8046_11378_1999	14	30	44	31.82
BS8231_25075_1998	6	11	17	35.29
BS8337_1223_1998	21	15	36	58.33
BS8402_25073_1999	10	42	52	19.23
BS8425_25074_1998	6	9	15	40.00
BS8477_15966_1999	3	25	28	10.71
BS8571_25076_1998	5	23	28	17.86
BS8591_25071_1998	13	25	38	34.21
BS9041_11376_2000	9	28	37	24.32
BS9064_25070_1999	3	3	6	50.00
BS9065_25072_1999	12	81	93	12.90
BS9067_25072_1998	9	28	37	24.32
BS9084_11377_1999	8	47	55	14.55
BS946_25070_1998	5	8	13	38.46
BS961_1223_1998	4	13	17	23.53
BS9884_25072_1999	8	48	56	14.29
BS9966_11376_1999	11	42	53	20.75
CF3142_25075_1998	22	79	101	21.78
CF4403_25075_1999	7	36	43	16.28
DB868_11378_2000	11	47	58	18.97

APPENDIX 2. OCEANOGRAPHIC DATA

We selected environmental variables on the basis of their biological relevance and availability for explaining the foraging habitat of the wandering albatross: dynamic oceanographic variables such as sea surface temperature (SST, as a proxy of water mass distribution), chlorophyll *a* concentration (CHL, as a proxy of biological production), and sea surface height (SSH, as a proxy of oceanic currents)(Louzao et al. 2011), and we also included wind speed (WIND) since it has been demonstrated that it is an important factor explaining movement patterns of wandering albatrosses (Weimerskirch et al. 2000, 2012). Dynamic variables were extracted from both data sources (OPA-PISCES model and satellite), whereas static variables such as bathymetry were obtained once from NOAA's ETOPO 2-minute dataset and its spatial gradient (BATG) was computed as the proportional change (PC) within a surrounding 3 x 3 cell grid using a moving window as follows: PC = [(maximum value - minimum value) * 100] / (maximum value). Finally, the distance to the colony was estimated in order to consider the influence of central place foraging (COLONY).

OPA-PISCES oceanographic data were based on the ORCA05 global configuration of the ocean general circulation model Nucleus for European Modelling of the Ocean-Océan Parallélisé (OPA-NEMO) (Madec 2008). The ocean general circulation model was then coupled with the ocean biogeochemical model PISCES, which has been successfully used to simulate and understand the dynamics of biogeochemical fields in the global ocean (Aumont et al. 2003, Aumont & Bopp 2006). The model has been described in detail in Aumont and Bopp (2006). Briefly, the ocean circulation model was coupled to the biogeochemical component estimating 24 different biogeochemical variables (e.g., nutrients, phytoplankton, and zooplankton). The coupled model of OPA-PISCES simulates oceanographic variables at a wide spectrum of spatial and temporal scales and the biological productivity of the ocean at a

1° spatial resolution from 1958 to 2001. Finally, we derived simulated wind speed (m s^{-1}) values based on zonal and meridional wind stress by the following equation (Large and Pond 1981):

$$Wind\ Speed = ((abs\ (Zonal_{\mathrm{stress}}) + \mathrm{abs}\ (Meridional_{\mathrm{stress}})) / 0.0014 / 1.22)^{0.5} \quad (1)$$

Remotely sensed oceanographic variables differed in spatial resolutions and were aggregated to match the standard grid of 1° cell size used by the OPA-PISCES simulations. We derived monthly composites of SST, CHL, SSH and WIND from PATHFINDER, SEAWIFS, AVISO and NOAA/NCDC Blended thanks to the Environmental Research Division's Data Access Program managed by the National Oceanic and Atmospheric Administration of USA, respectively (available at BloomWatch with a spatial resolution of ca. 0.04°, 0.1°, 0.25° and 0.25°; http://coastwatch.pfel.noaa.gov/coastwatch/CWBrowserWW180.jsp). Data were obtained from 1998 to 2001.

Oceanographic conditions during the overlap time window (1998-2001)

During the validation period (January-December 1998-2001), the Southern Indian Ocean was characterized by a mean surface temperature of 7.91°C (based on satellite values), ranging from 26.8°C in tropical waters to -1.7°C in the Antarctic area. Mean monthly values showed a marked latitudinal gradient which was evidenced year-round, even if some areas showed higher SST variability (higher values of SD in the northwest in January; 1998-2001) related to the dynamic Agulhas Current (Fig. A1.1a). Regarding ocean productivity, chlorophyll *a* concentration was on average 0.27 mg m-^{3}, ranging from oligotrophic to enriched waters (range: 0.03 - 28.09). During the incubation period, the maximum CHL concentration was found east of Kerguelen, as well as maximum variability (Fig. A1.1b). Mean sea surface height was 0.95 cm, increasing from Antarctic to tropical waters (range: -0.39 - 2.87) and showing similar patterns to SST (i.e. both similar latitudinal gradients and areas of inter-annual SSH variability associated to the Agulhas Current; standard deviation values of Figs. A1.1a and A1.1c). Finally, the mean wind speed was 10 m s^{-1} (range: 1.40 - 30.14) and the averaged map showed an important latitudinal band where wind speed was more intense, between 45°-60°S (Fig. A1.1d).

References

Aumont, O. et al. 2003. An ecosystem model of the global ocean including Fe, Si, P colimitations. - Global Biogeochem. Cycles 17: 1060, doi:10.1029/2001 GB001745.

Aumont, O. and Bopp, L. 2006. Globalizing results from ocean in situ iron fertilization studies. - Global Biogeochem. Cycles 20: GB2017.

Large, W. G. and Pond, S. 1981. Open ocean momentum flux measurements in moderate to strong winds. – J. Phys. Oceanogr. 11: 324-336.

Louzao, M. et al. In press. Conserving pelagic habitats: seascape modelling of an oceanic top predator. – J. Appl. Ecol.

Madec, G. 2008 NEMO reference manual, ocean dynamics component: NEMO-OPA, volume 27. - Note du Pole de modélisation, Institut Pierre-Simon Laplace (IPSL) 27.

Weimerskirch, H. et al. 2000. Fast and fuel efficient? Optimal use of wind by flying albatrosses. - Proc. R. Soc. Lond. B 267: 1869-1874.

Figure A2.1. Mean (± SD) oceanographic conditions during the validation period (January, 1998-2001), measured by both satellite and model datasets: (a) sea surface temperature (°C), (b) chlorophyll (mg m^{-3}), (c) sea surface height (cm) and (c) wind speed (m s^{-1}). Note the high correlation for SST, SSH and WIND (Spearman-rank correlation coefficient for SST: r_s = 0.989, $P < 0.001$; for SSH: r_s = 0.973, $P < 0.001$; for WIND: r_s = 0.886, $P < 0.001$), contrary to the weak correlation for the CHL (r_s = 0.315, $P < 0.001$).

(a)

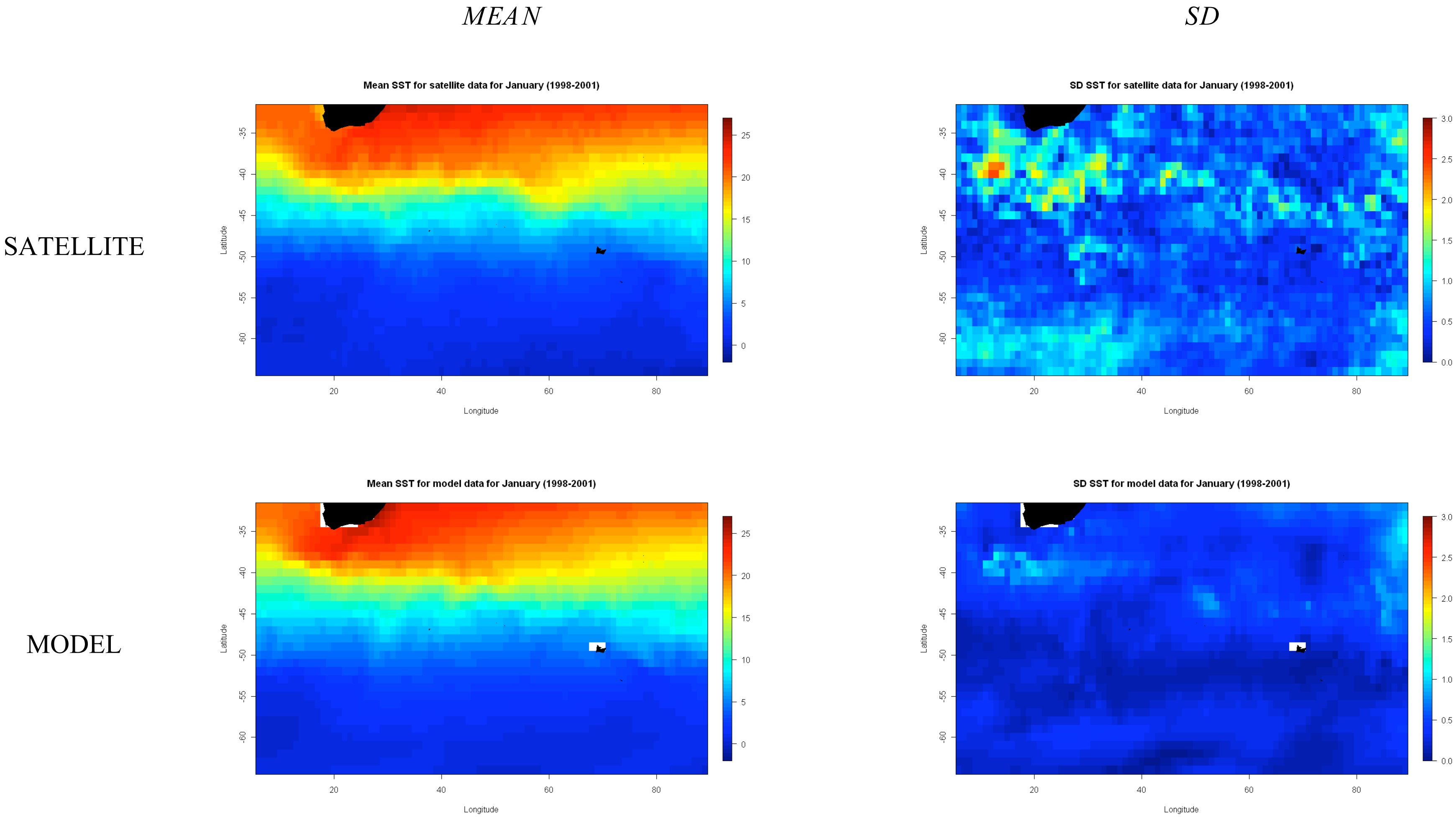
MEAN
SD
SATELLITE
MODEL
Mean SST for satellite data for January (1998-2001)
SD SST for satellite data for January (1998-2001)
Mean SST for model data for January (1998-2001)
SD SST for model data for January (1998-2001)
Latitude
Longitude
-35
-40
-45
-50
-55
-60
20
40
60
80
0
5
10
15
20
25
0.0
0.5
1.0
1.5
2.0
2.5
3.0

(b)

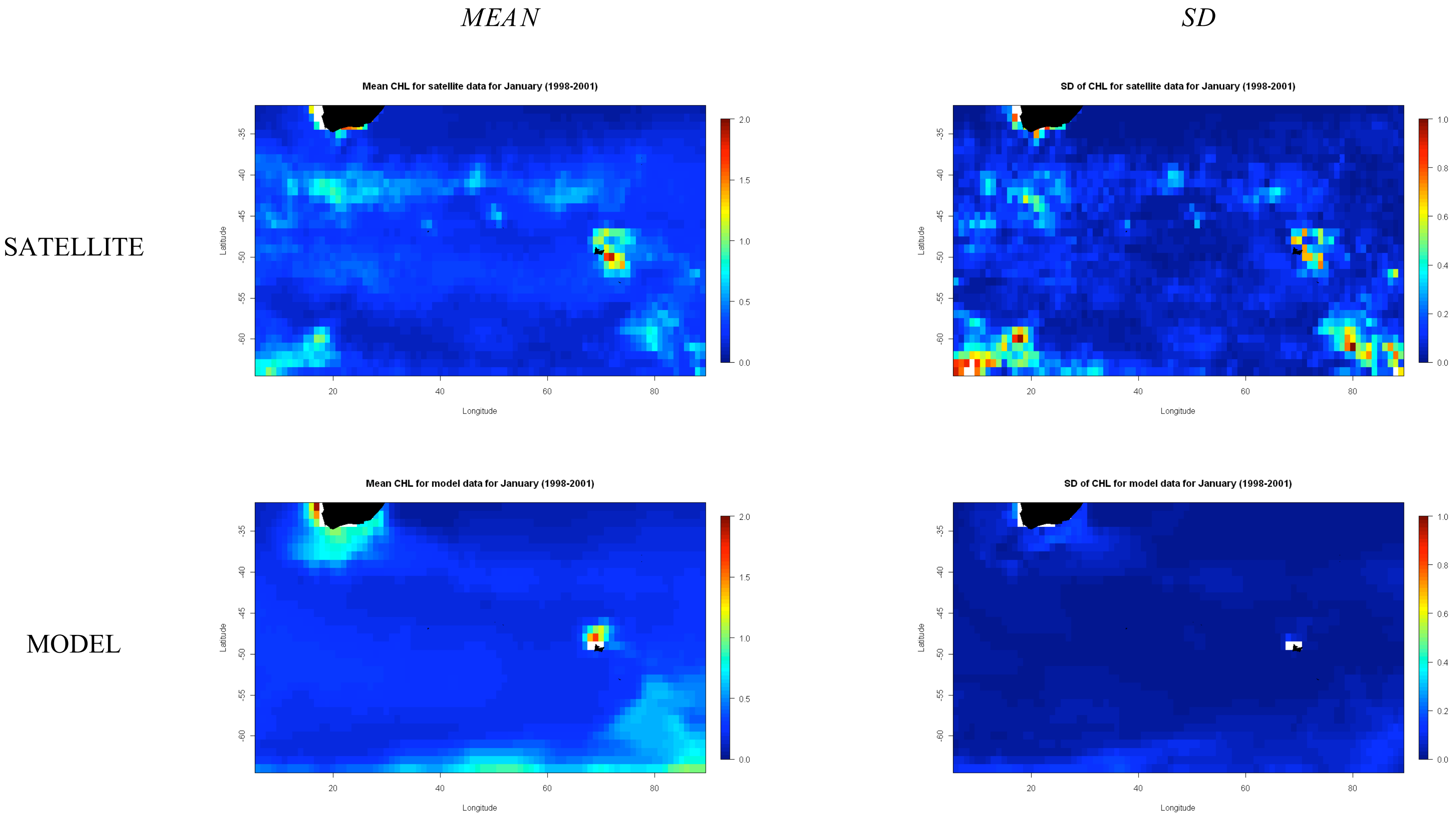

MEAN
SD
SATELLITE
MODEL
Mean CHL for satellite data for January (1998-2001)
SD of CHL for satellite data for January (1998-2001)
Mean CHL for model data for January (1998-2001)
SD of CHL for model data for January (1998-2001)
Latitude
Longitude
-35
-40
-45
-50
-55
-60
20
40
60
80
0.0
0.5
1.0
1.5
2.0
0.2
0.4
0.6
0.8

(c)

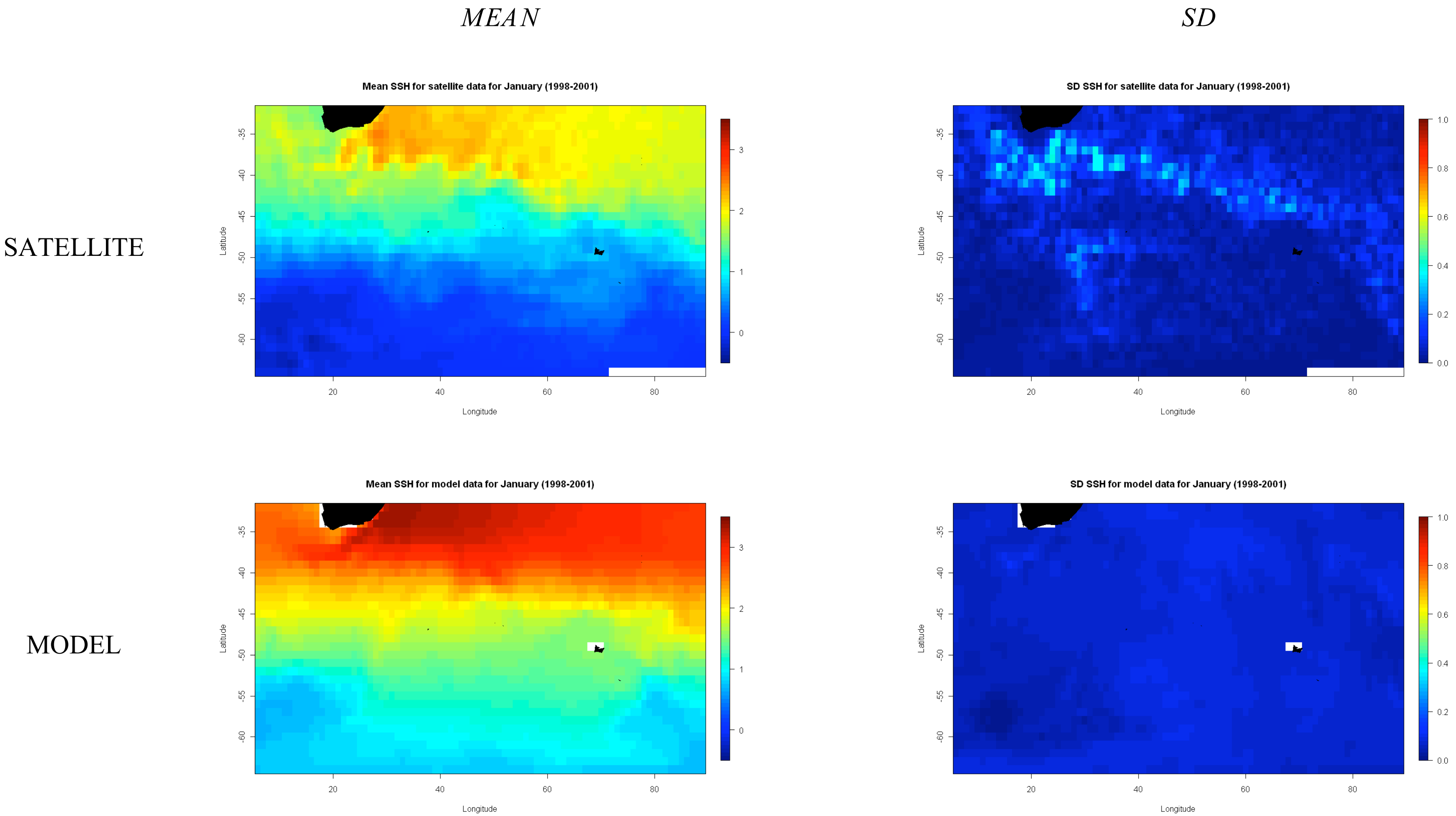

MEAN
SD
SATELLITE
MODEL
Mean SSH for satellite data for January (1998-2001)
SD SSH for satellite data for January (1998-2001)
Mean SSH for model data for January (1998-2001)
SD SSH for model data for January (1998-2001)
Latitude
Longitude

(d)

MEAN *SD*

SATELLITE

MODEL

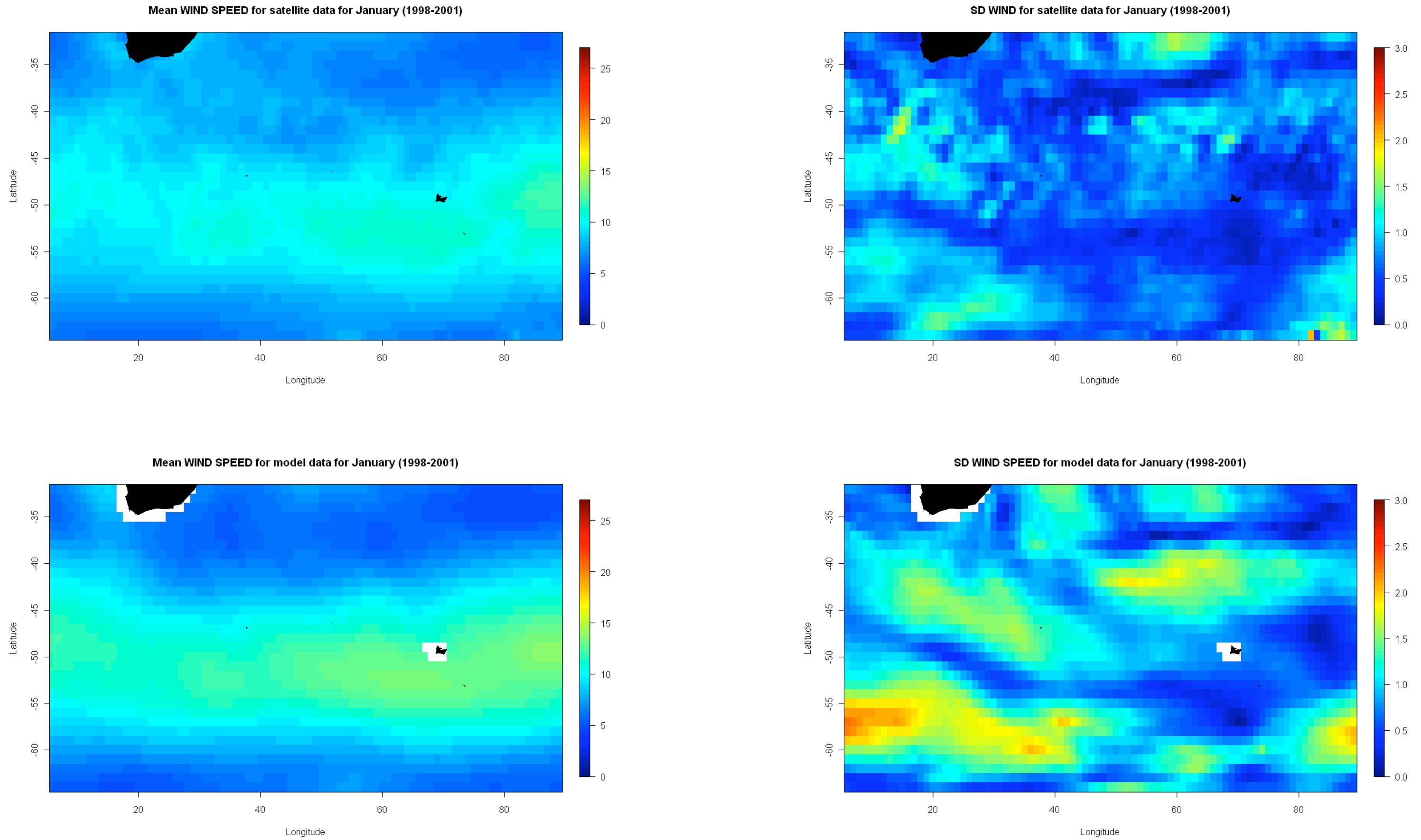

.

Figure A2.2 Validation of OPA-PISCES oceanographic information by contrasting satellite and model datasets in the same spatio-temporal resolution for the validation period (48 months: 1998-2001): (a) sea surface temperature (°C; SST), (b) chlorophyll (mg m^{-3}; CHL), (c) sea surface height (cm; SSH) and (d) wind speed (m s^{-1}, WIND). Note the high correlation for SST, SSH and WIND (Spearman-rank correlation coefficient for SST: $r_s = 0.989$, $P < 0.001$; for SSH: $r_s = 0.973$, $P < 0.001$; for WIND: $r_s = 0.886$, $P < 0.001$), contrary to the weak correlation for the CHL ($r_s = 0.315$, $P < 0.001$).

(a)

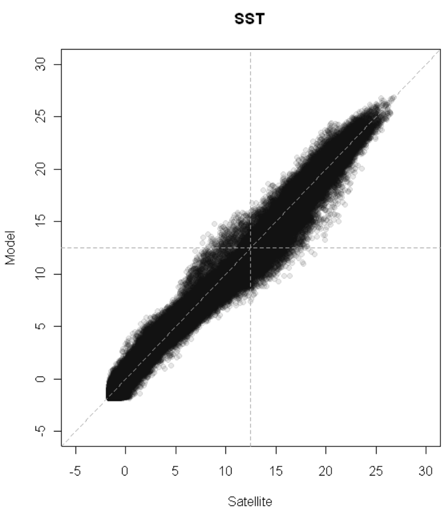

(b)

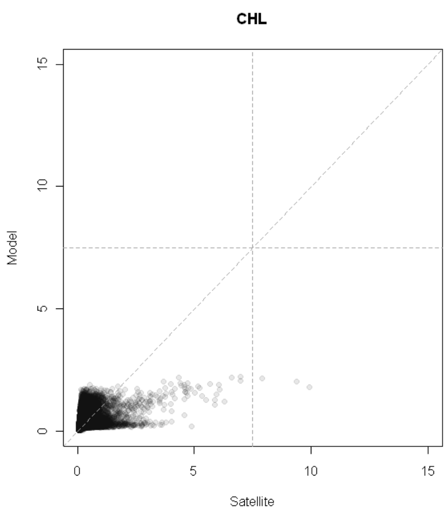

(c)

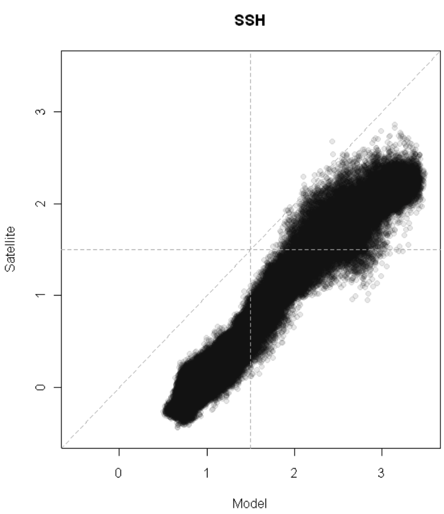

(d)

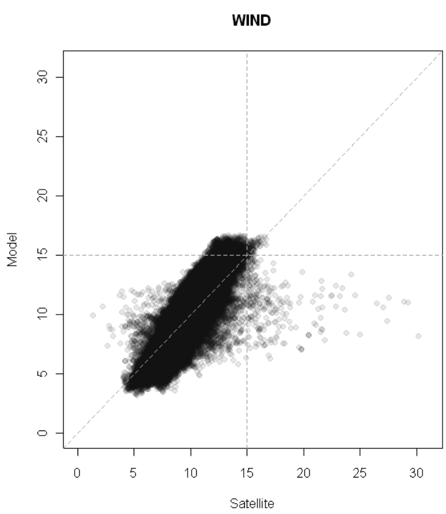

Figure A2.3. Validation of OPA-PISCES oceanographic information by contrasting both satellite- and model-based datasets at the same spatiotemporal resolution for the validation period (48 months: 1998-2001): (a) sea surface temperature (°C; SST), (b) chlorophyll *a* (mg m^{-3}; CHL), (c) sea surface height (m; SSH) and wind speed (m s-1; WIND). Note the high correlation for SST, SSH and WIND (Spearman-rank correlation coefficient for SST: r_s = 0.989, $P < 0.001$; for SSH: r_s = 0.973, $P < 0.001$; for WIND: r_s = 0.886, $P < 0.001$), contrary to the weak correlation for the CHL (r_s = 0.315, $P < 0.001$).

a

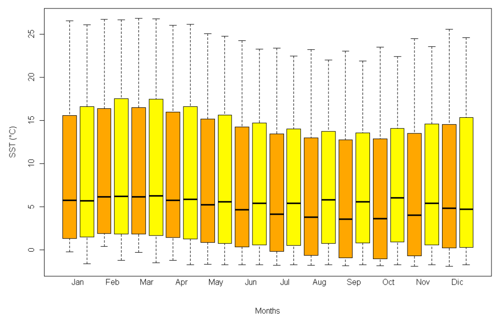

b

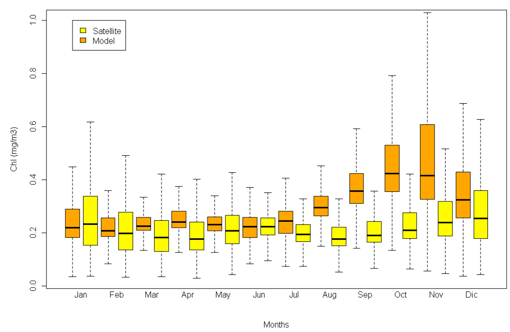

c

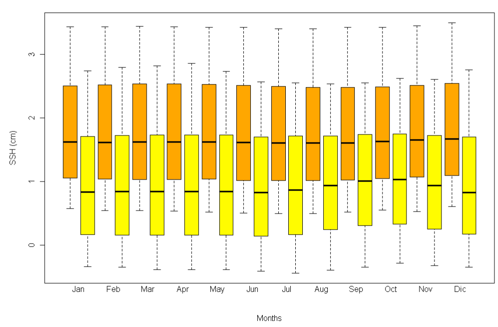

d

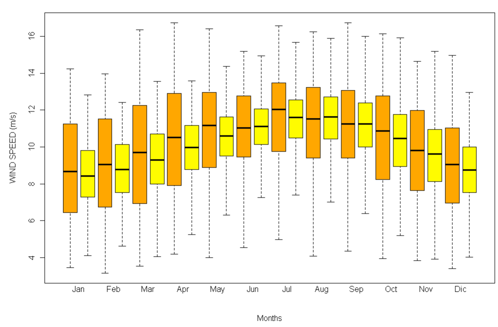

Figure A2.4. Differences between mean satellite- and model-based chlorophyll *a* concentration (mg/m^3) for the validation period during (a) January, (b) February and (c) March (1998-2001).

(a)

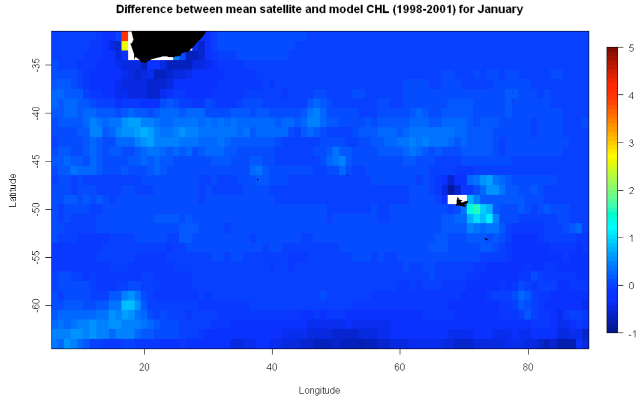

(b)

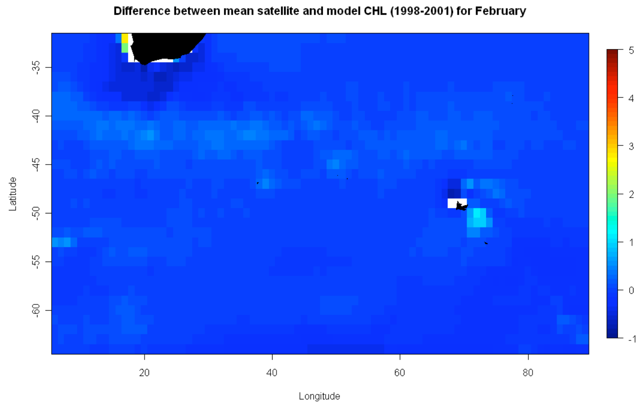

(c)

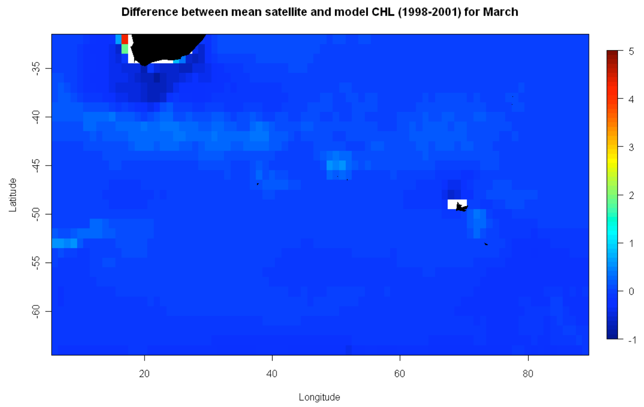

APPENDIX 3. MODELLING OUTPUT

Figure A3.1**.** Model evaluation of Wandering Albatross foraging patterns. (a) The out-of-bootstrap distribution of the negative log-likelihood is given for models considering dynamic satellite-based and OPA-PISCES based variables plus static data, respectively. (b) Satellite based versus OPA-PISCES based foraging probability. (c) Comparison of the out-of-bootstrap distribution of the negative log-likelihood of the constant null model and final model for OPA-PISCES based modelling.

(a)

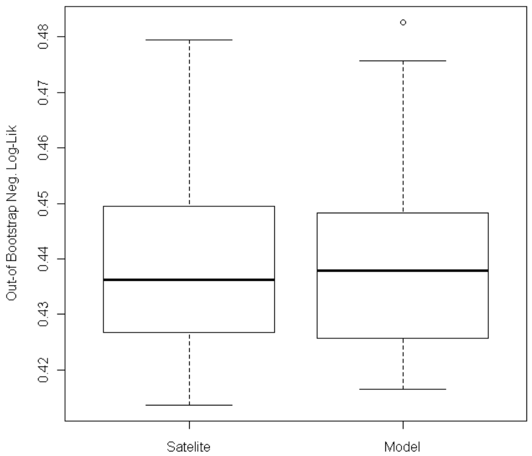

(b)

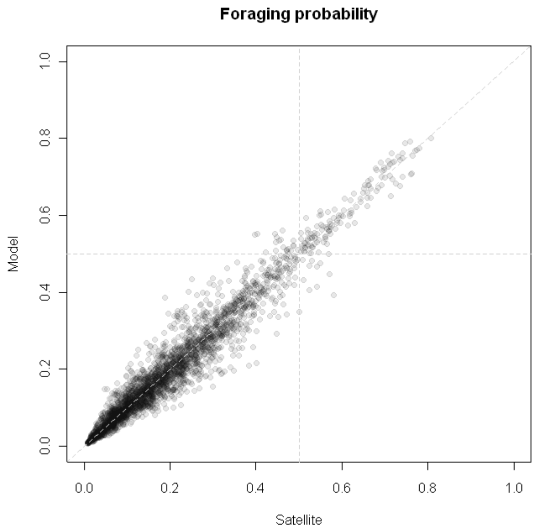

(c)

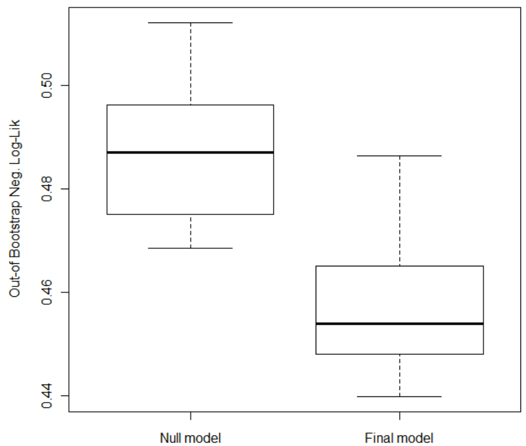

Figure A3.2. Partial effects of dynamic satellite parameters (left column), static variables (central column) and both random and spatial components (right column) on wanderers foraging probability.

(a)

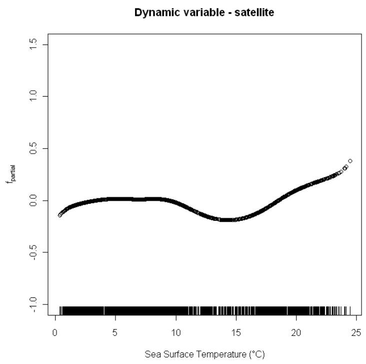

(b)

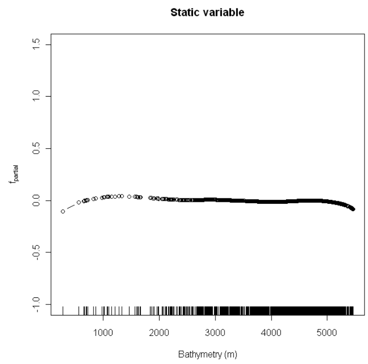

(c)

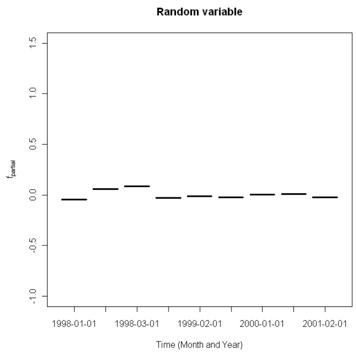

(d)

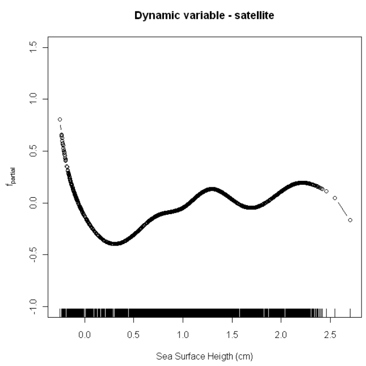

(e)

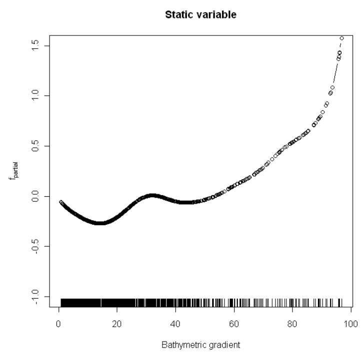

(f)

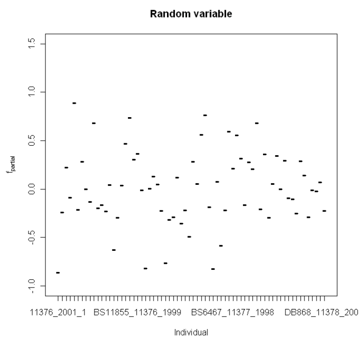

(g)

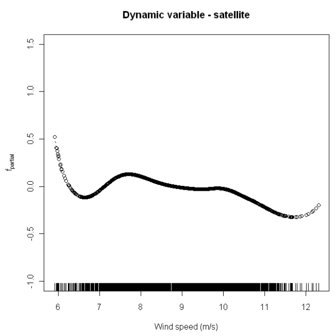

(h)

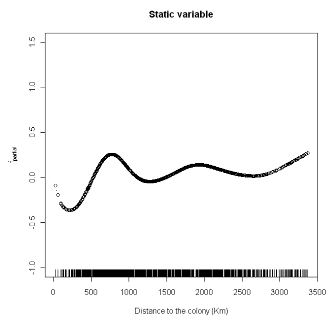

(i)

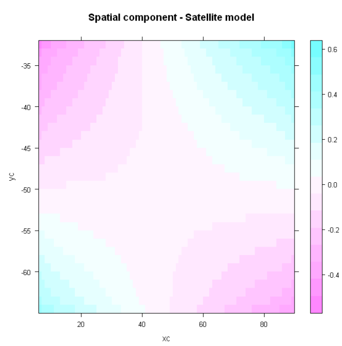

Figure A3.3. Spatial component for females based on (a) satellite and (b) OPA-PISCES parameters.

(a)

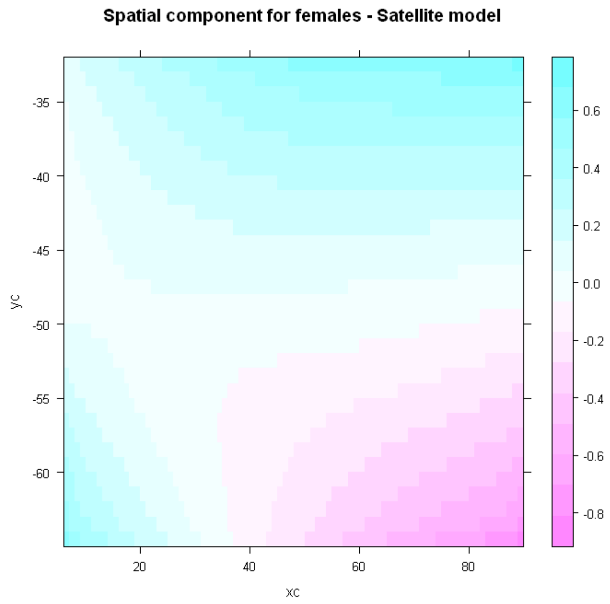

(b)

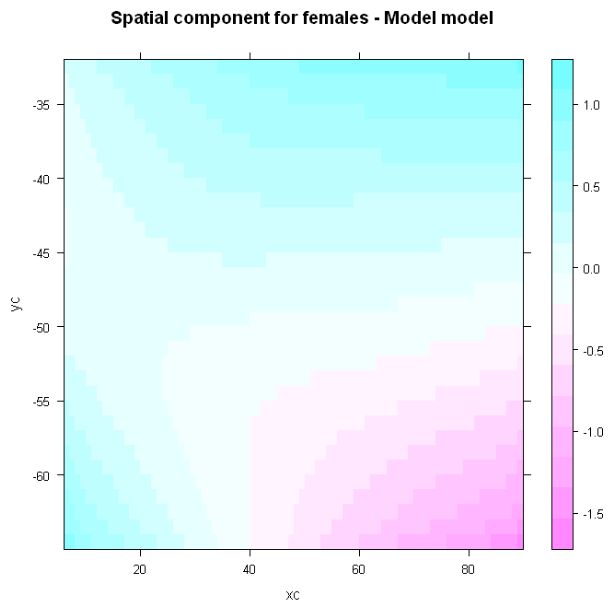

Figure A3.4. Partial effects of dynamic OPA-PISCES parameters (left column), static variables (central column) and both random and spatial components (right column) on wanderers foraging probability.

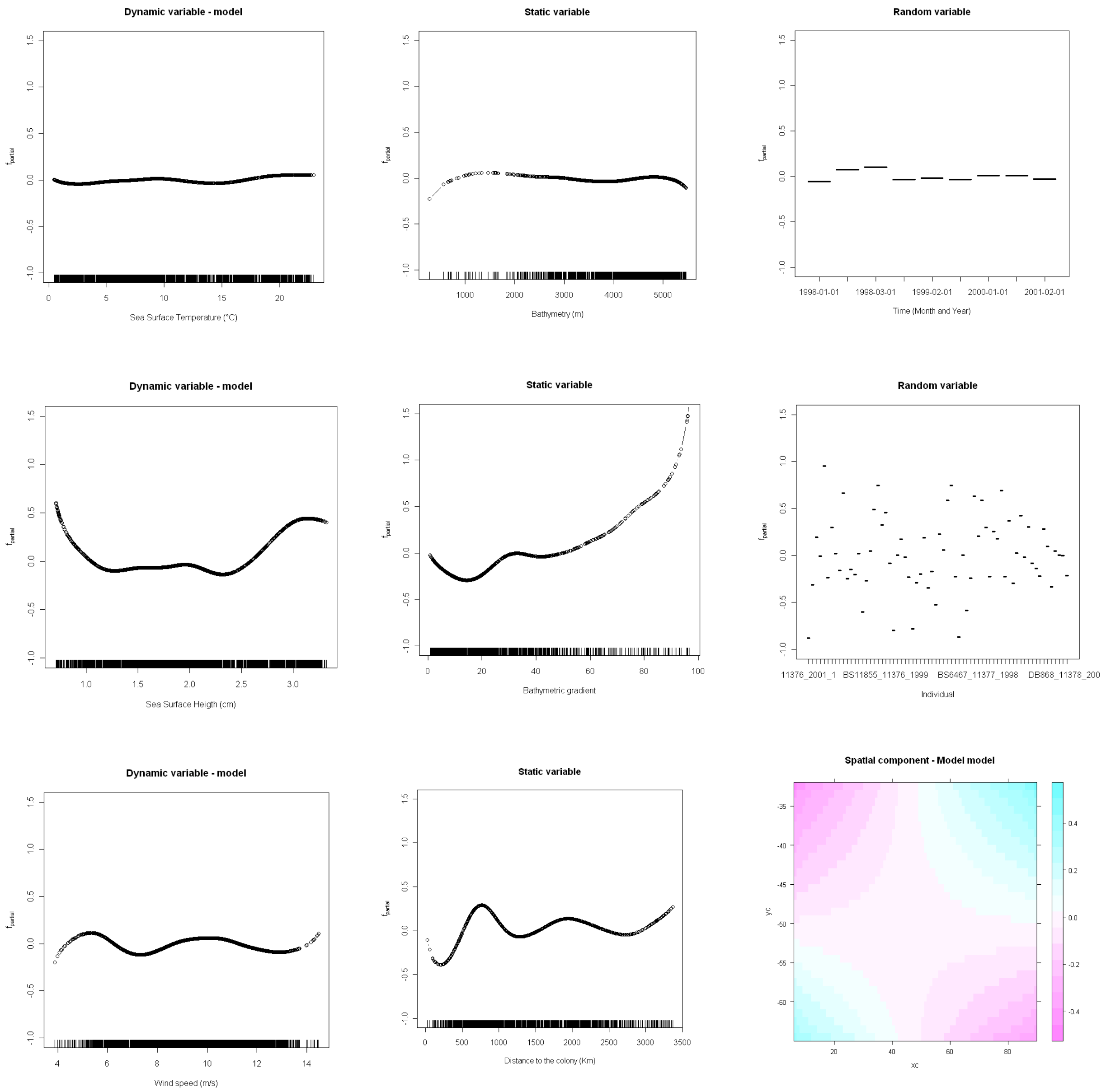

Figure A3.5. Satellite-based and model-based spatial predictions for January 1998-2001.

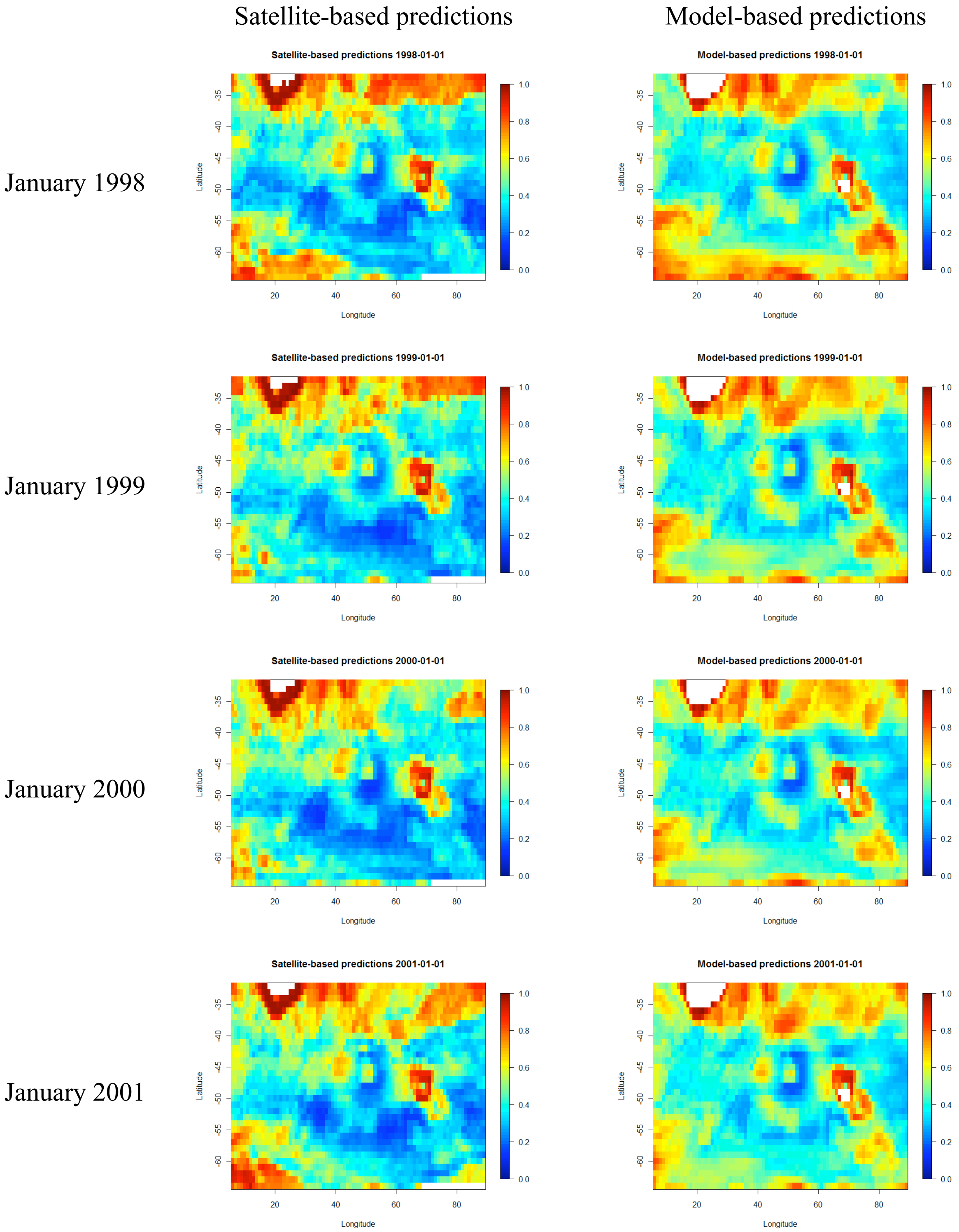

APPENDIX 4. HISTORICAL FORAGING HABITATS

Figure A4.1. Mean (± SD) predictions of the foraging probability (left and right panel, respectively) during January, February and March over the 44-years study period (1958-2001). The right scale bar indicates mean foraging probability (from 0 to 1) or SD (from 0 to 0.25). Black contour lines represent the isobaths of 200 m, 1000 m and 3000 m. The white square represents the marine area from which foraging predictions was extracted for further interpret their temporal evolution.

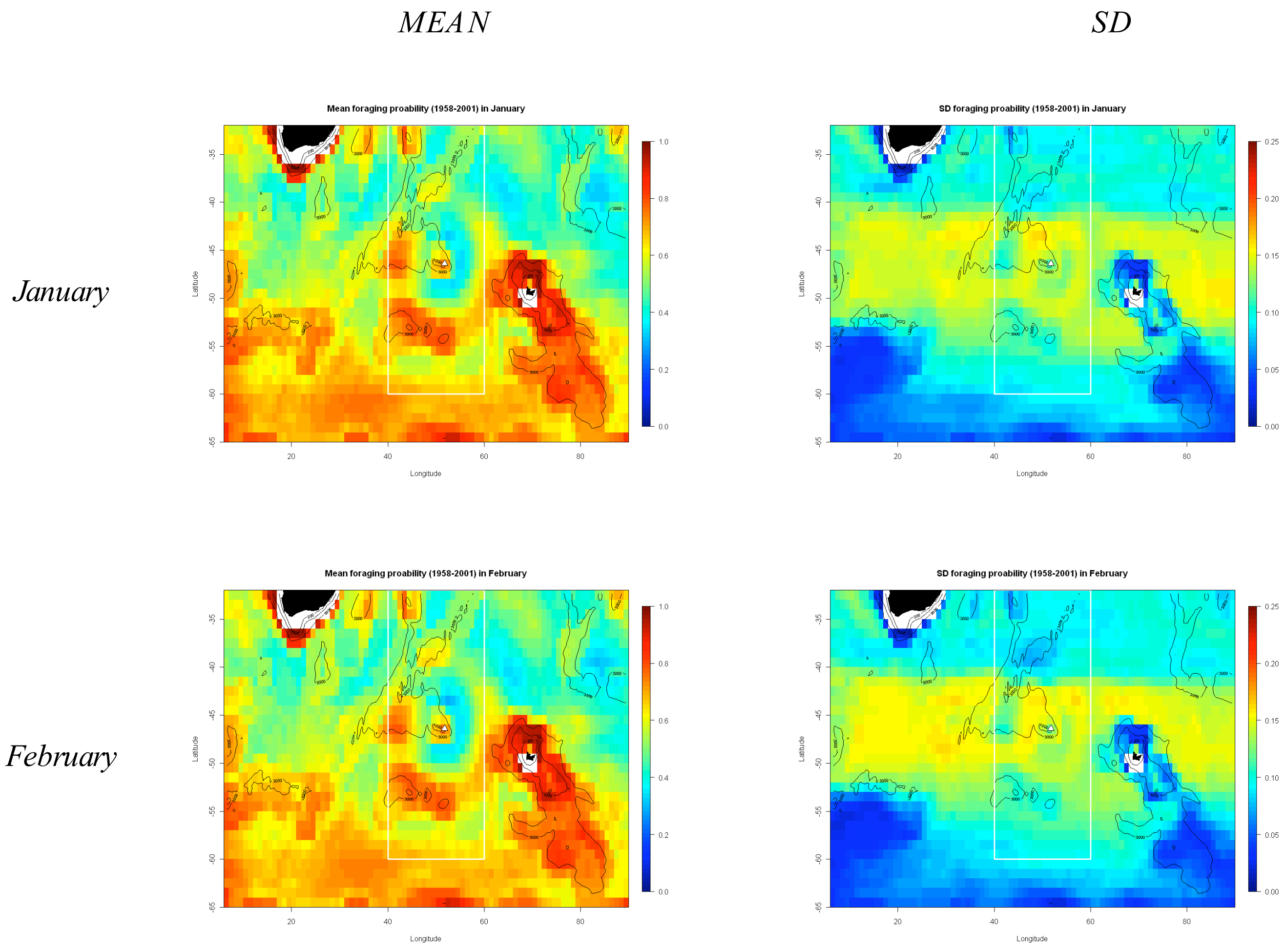

March

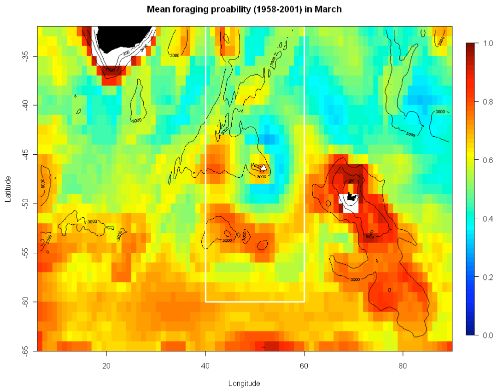

Mean foraging proability (1958-2001) in March
Latitude
Longitude

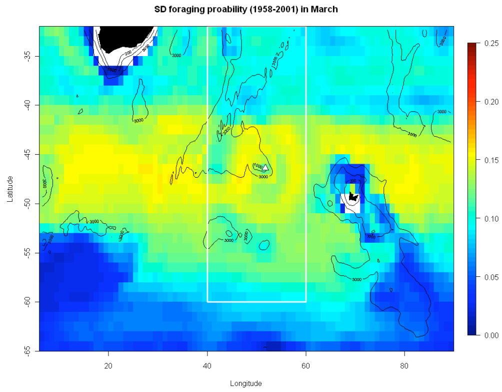

SD foraging proability (1958-2001) in March
Latitude
Longitude

Figure A4.2. Temporal evolution of (a) sea surface temperature, (b) sea surface height and (c) wind speed from 1958 to 2001 at Crozet (black lines) and northern, central and southern band of latitude (30°-40°S, 40°-50°S and 50°-60°S represented by (green, red and blue lines, respectively) averaged over 40°-60°E, respectively). Solid lines indicate average values for the incubation period, whereas the three dotted lines represent average values for January, February and March.

(a)

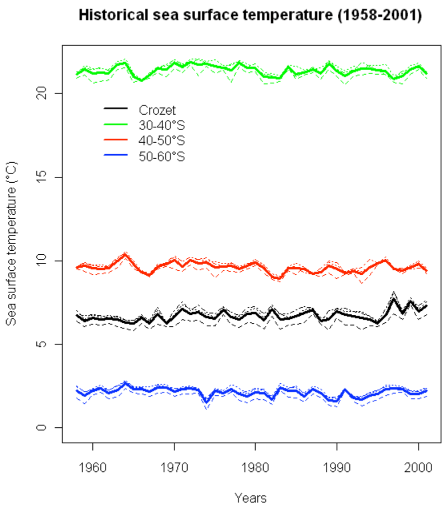

(b)

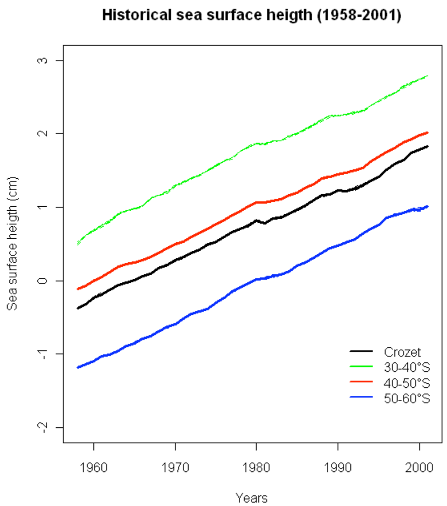

(c)

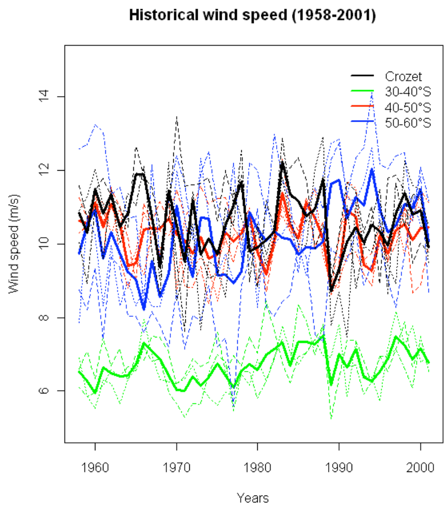

Figure A4.3. Temporal evolution of (a) sea surface temperature (°C, SST), (b) sea surface height (cm, SSH) and (c) wind speed (m s^{-1}, WIND) from 1958 to 2001. Figures represent averaged values over 40°-60°E from latitude 32°S to 60°S. The white dotted line indicates the latitude of Crozet. Contour (black) lines guide the temporal evolution of different parameter values.

(a) (b) (c)

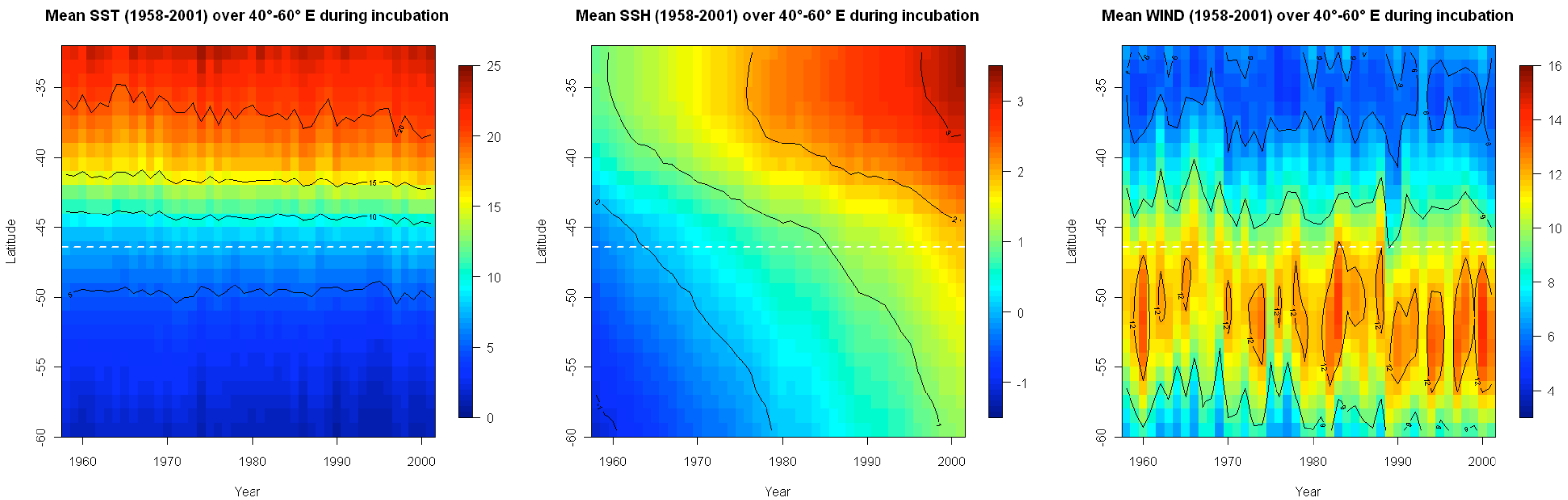

Figure A4.4. Animations showing the historical evolution (1958-2001) of (a) foraging probability (ForProb) of Wandering Albatrosses and dynamic environmental variables such as (b) sea surface temperature (°C, SST), (c) sea surface height (cm, SSH) and (d) wind speed (m s^{-1}, WIND) in the southern Indian Ocean during the 3-month (January, February and March) incubation period. Animations were built in Shockwave Flash (*.swf). A free player can be downloaded from http://www.show-kit.com/flash-player/.

(a)

ForProb_January.swf ForProb_February.swf ForProb_March.swf

(b)

SST_January.swf SST_February.swf SST_March.swf

(c)

SSH_January.swf SSH_February.swf SSH_March.swf

(d)

WIND_January.swf WIND_February.swf WIND_March.swf